ISSN 0030-400X, Optics and Spectroscopy, 2014, Vol. 117, No. 3, pp. 480–485. © Pleiades Publishing, Ltd., 2014.

PHYSICAL OPTICS

Combined Optical Dispersion by Prism and Arrayed Waveguide Grating with Multiple Diffraction Orders for Raman Spectrometer[1]

Ya-qin Cheng[a], Hong-da Sun[a], Zhao Wu[a], Sheng-feng Deng[b], and Miao Lu[b]*

[a] *MEMS Research Center, Xiamen University, Xiamen, China*

[b] *Pen-Tung Sah Micro-Nano Technology Institute, Xiamen University, Xiamen, 361005 China*

**e-mail: lm@xmu.edu.cn*

Received January 25, 2013

Abstract—A compact dispersive device for Raman spectrometer was proposed to achieve a spectrum resolution below 0.55 nm in the spectral range of 800 to 1000 nm. A 41-channel arrayed waveguide grating (AWG) with eleven different diffraction orders was designed, and each output channel of this AWG contained eleven light signals with periodically 20 nm spaced wavelength. These signals were further cross-dispersed by a prism, and finally form a 41 × 11 spots array on a CCD. The detailed theoretical analysis and simulation of this dispersive device were introduced in this paper. Compared with commercial dispersive modules composed of grating, lens, and mirrors, the proposed structure is able to provide a compact device with higher spectrum resolution, which is attractive for handheld Raman spectrometer.

DOI: 10.1134/S0030400X14090288

INTRODUCTION

Raman spectroscopy is able to detect chemical or biological molecules even with H_2O or CO_2 existence, and co-existing chemicals can be identified simultaneously according to their unique characteristic spectral peaks. So Raman spectroscopy is believed to be a kind of simple, speedy and powerful detection tool to identify chemicals in environment, food and drugs. However, the applications of Raman spectroscopy nowadays are severally limited by the expensive and bulky spectrometer. Theoretically, the spectral resolution of a traditional spectrometer composed of lens, mirrors and grating will drop significantly with its size scaled down. So some new architecture must be employed for low coat and compact Raman spectrometer. Meanwhile, arrayed waveguide grating (AWG) has been regarded as a substitute of bulky dispersive system, and was used successfully as a wavelength demultiplexer in optical communication system. AWG is prepared by micro fabrication technology and realizes the optical dispersive function on a chip, so a low-cost, handheld Raman spectrometer can probably be developed based on this compact dispersive chip.

Some AWG designs had been reported for spectrometer applications. Y. Komai et al. reported a compact spectroscopic sensor using a visible range 8 channel AWG [1]. K. Kodate et al. developed a hybrid chip integrating AWG device, laser diode and detector array to detect the concentration of chlorophylls in water, and an 8 channel AWG with 12.5 nm spectral resolution and 800 nm central wavelength was demonstrated with less than 4 dB insert loss [2]. P. Cheden et al. prepared an 8 × 8 mm^2, 50 channel AWG dispersive chip on SOI substrate, and its spectral resolution reached 0.2 nm at a central wavelength about 1545 nm [3]. N. Ismail et al. reported a 55 channel AWG with 800–920 nm spectral range on silicon-oxynitride waveguide to in-vivo detect the water concentration in human's skin [4]. N. Cvetojevic et al. utilized an AWG for astronomy to observe atmospheric molecular OH emission lines, and the demonstrated AWG had a free spectral range (FSR) of 57.4 ± 0.6 nm and a spectral resolution of 0.75 nm [5]. V.D. Nguyen et al. designed and fabricated an AWG based Optical Coherence Tomography, and the AWG has a footprint of 3.0 cm × 2.5 cm, operates at a center wavelength of 1300 nm, and has a FSR of 78 nm [6]. L. Chang et al. investigated another optical coherence tomography with an AWG center on 800 nm and a FSR of 19.4 nm [7]. Recently, S. Murugkar et al. developed an on-chip miniature AWG spectrometer based on slow light to realize high spectral resolution [8]. N. A. Yebo et al. integrated a 16 channel, 200 GHz (1.6 nm) space AWG with a micro-ring resonator for gas sensing [9, 10]. AWG with asymmetric structure was proposed by M. Pollnau's group in order to obtain low phase error and low insert loss [11–14]. However, all these reported AWG devices didn't exhibit a competitive performance with commercial portable Raman spectrometers, mainly due to high resolution and broad spectral range came at the cost of high insert loss and large device size for AWG.

Spectral range of a Raman spectrometer normally covers several hundred nanometers, so hundreds of

[1] The article is published in the original.

output channels were required to get a typical spectral resolution below 1 nm. A low diffraction order m and a reduced increment (ΔL) of the arrayed waveguide below 10 μm are unavoidable, and the layout of such an AWG is hard to draw using widely used commercial AWG design tools because of the overlapping of consecutive waveguides. Even if the layout can be constructed, its footprint will be too large to be fabricated in a wafer with an acceptable yield.

Cascaded AWG configurations were proposed in recent literatures to realize broadband, high-resolution spectrometers. K. Takada et al. reported a 1010-channel cascaded AWG filter with 10 GHz channel spacing, wherein a 10-channel AWG acted as the pre-stage to assign lights into ten 160-channel second-level AWGs, but the insert loss was up to 13 to 19 dB [15]. B. Momeni et al. proposed a cascaded structure consisting of a low resolution and wideband AWG as the first stage, followed by high resolution super-prism devices based on photonic crystals [16], and this kind of super-prism was discussed in details in several other papers published by the same group [17–19]. B. Momeni et al. also demonstrated another cascaded configuration including an AWG followed by a set of resonators, experimental results showed the capability of such spectrometer to achieve ~0.1 nm wavelength resolution over 10 nm bandwidth in a compact device in millimeter scale [20]. However, a cascaded AWG system normally had an insert loss more than 10 dB and a non-uniform passband, which hindered its application in Raman spectrometer. In recent, B.I. Akca et al. presented a new synchronized design for flattening the passband of a cascaded AWG system, which consisted of the low-loss flat-top AWG as a primary filter and five 1×51 AWGs with a 0.4-nm channel spacing as secondary filters, but the overall insert loss was still high [21].

Another approach to realize broadband and high spectral resolution simultaneously is to adopt multiple diffraction orders. In this case, multiple overlapping lights with periodically spaced wavelength were contained in each output waveguide. N. Ismail et al. prepared an AWG with multi-order overlapped spectrum to test human's teeth containing localized initial carious lesions, and achieved a spectral range of 859–957 nm and a resolution of 0.2 nm [22]. Unfortunately, these multiple lights in an output waveguide must be further dispersed in most spectrometer applications. J. Bland-Hawthorn et al. developed an integrated cross-dispersive optics to avoid overlapping of lights from the same output channel, and succeed to identify the optical signals from an astronomical telescope in a wide spectral range. However, the cross-disperser was not discussed in details in the papers [23, 24]. In an illustration figure, the lights are focused by a micro cylinder lens before being cross-dispersed by a micro prism, but lateral overlapping of lights from adjacent output channels will probably occur.

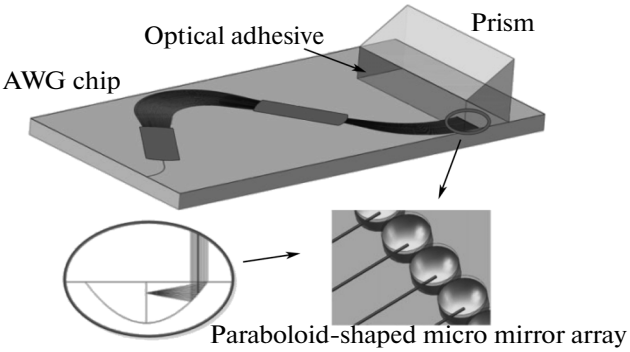

Fig. 1. The illustration of the structure of the proposed dispersive device.

In this paper, a new cross-disperser for a multi-order AWG was proposed for broadband Raman spectrometer. This cross-disperser consisted of a parabolic-shaped micro mirror array and a prism, this micro mirror array was fabricated on the same chip with AWG, and the prism was glued on the chip by optical adhesive. As a demonstration of this concept, a dispersive device with 800–1000 nm range and about 0.55 nm spectral resolution was designed and simulated, it can be realized in a volume of several cubic centimeters and is promising for handheld Raman spectrometers.

CONCEPT OF THE DISPERSIVE DEVICE

As shown in Fig. 1, the proposed dispersive device consists of three components: an AWG chip, a prism and a parabolic-shape micro mirror array. The AWG in this configuration worked on multiple diffraction orders, and contained multiple lights with periodically spaced wavelength in each output waveguide. A parabolic-shape mirror array was built, and the end of each output waveguide of the AWG located exactly at the focal point of the parabolic-shape mirror. Therefore, the light from each output waveguide was reflected upwards and collimated. A prism with high index of refraction (PS851, Thorlabs Co., USA) was glued on the AWG wafer using a kind of optical adhesive (NOA13685, Norland Co., USA) in the way that one of its surface was set close to the ends of output waveguide of AWG. In this configuration, the lights in the same output waveguide were cross-dispersed by this prism.

DESIGN AND SIMULATION OF AWG WITH MULTIPLE DIFFRACTION ORDER

AWG Based on Silicon Oxynitride Waveguide

An AWG with multiple diffraction orders was designed based on silicon oxynitride waveguide. Through changing the flow rate of SiH_4 and N_2O in the deposition process, silicon oxynitride with refractive index of 1.483 and 1.468 was prepared to act as the core and cladding layer, respectively. The layout of the

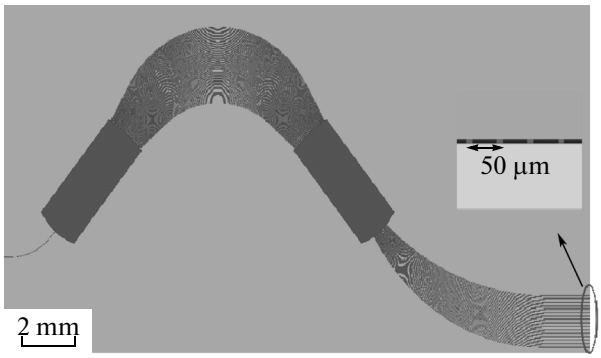

Fig. 2. The layout of the AWG with eleven diffraction orders based on silicon oxynitride waveguide.

AWG was shown in Fig. 2, here the footprint of the 41 channel AWG is 23 mm × 14 mm and the cross-section of waveguide is about 2 μm × 1.5 μm.

The Determination of Diffraction Order

Just like other kinds of grating, an AWG also has the spectral periodicity. When a beam with a wide spectral range such as a Raman scattering light propagates through an AWG, lights with different wavelength gathers at the same output channel.

According to the grating equation, the diffracted light has to satisfy Eq. (1)

$$\sin\theta_i d_a n_s(\lambda_i) + \sin\theta_o d_a n_s(\lambda_i) + n_c(\lambda_i)\Delta L = m\lambda, \quad (1)$$

where θ_i is the input angle, θ_o is the output angle, λ_i is the input wavelength, d_a is the arrayed waveguide pitch, ΔL is the length increment between adjacent arrayed waveguides, m is the corresponding diffraction order for input wavelength, $n_s(\lambda_i)$ and $n_c(\lambda_i)$ are the effective refractive index of free propagation region (FPR) and arrayed waveguides, and they are a function of input wavelength.

The central wavelength λ_{cm} with corresponding diffraction order m is determined in Eq. (2)

$$n_c(\lambda_{cm})\Delta L = m\lambda_{cm}. \quad (2)$$

Table

Parameters	
Arrayed waveguide increment ΔL, μm	29.592
FPR length f, μm	4930
Channel number, N	41
Number of array waveguide	168
The pitch of output waveguide Δx, μm	9
The pitch of arrayed waveguides d, μm	9
Chip size, mm^2	25 × 13

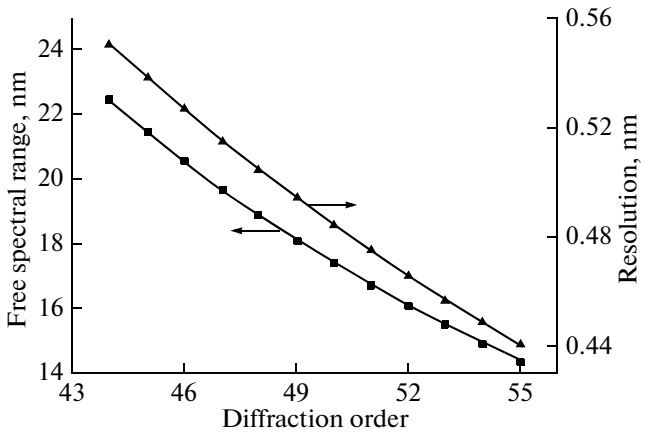

Fig. 3. The relationship of spectral resolution (tviangles) and free spectral range (squares) versus diffraction order.

The FSR is defined as wavelength range between two adjacent diffraction peaks and solved by Eq. (3)

$$\mathrm{FSR} = \frac{\lambda_{cm} n_c(\lambda_{cm})}{m n_g(\lambda_{cm})} = \frac{\Delta L n_c(\lambda_{cm})^2}{m^2 n_g(\lambda_{cm})}, \quad (3)$$

where n_g is the group index and defined as $n_g = n_c - \lambda dn_c/d\lambda$.

The spectral resolution $\Delta\lambda_m$ for the matching diffraction order m will be determined by Eq. (4)

$$\Delta\lambda_{\mathrm{m}} = \frac{d\lambda}{d\theta}\Delta\theta = \frac{n_s d_a n_c}{m n_g}, \quad (4)$$

where Δx_o is the pitch of output waveguides and f is the focal length of FPR.

In Eq. (3), FSR is inversely proportional to the second power of m, while in Eq. (4), $\Delta\lambda_m$ is inversely proportional to m. Accordingly, the relationship between FSR, $\Delta\lambda_m$ and the diffraction order m were shown in Fig. 3.

In order to form a continuous spectrum, the individual spectrum range of adjacent diffraction order should be a little bit overlapped. Considering the required spectral resolution below 0.55 nm, the maximum FSR must be larger than multiplying 0.55 nm by the channel number, 41, and the product was about 22 nm. So the diffraction order m was determined to be 44 to 54 in Fig. 3. Here, the central wavelength corresponding to $m = 44$ was 990 nm.

Optimization of AWG Parameters

Table showed the final parameters of the AWG. Because low insert loss is essential for Raman spectrometer, a large pitch of arrayed waveguides and output waveguides were chosen. Furthermore, linear taper waveguides were introduced in the junction between slab waveguide and strip waveguides to reduce the insert loss.

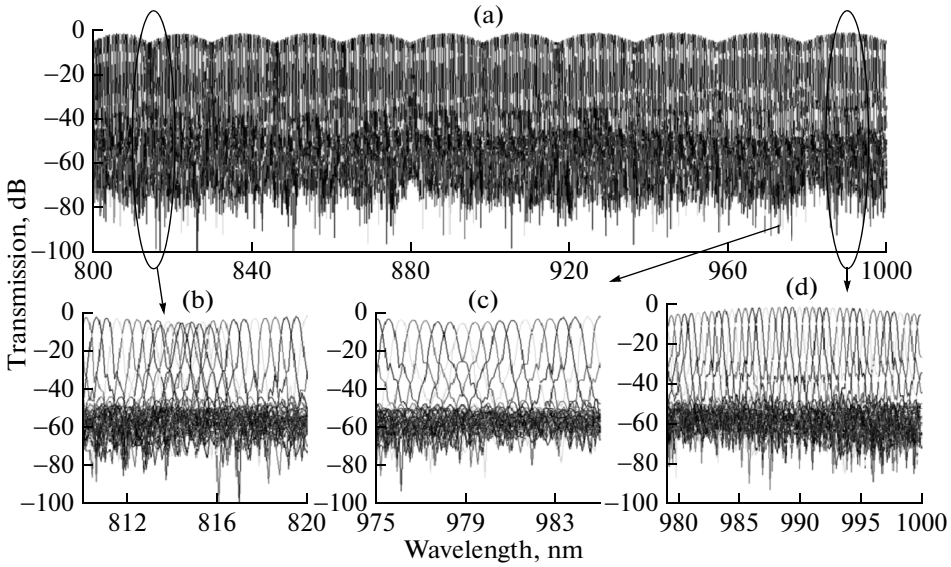

Fig. 4. The simulated transmission of the AWG with multiple diffraction orders: (a) the transmission from 800 nm to 1000 nm with eleven diffraction orders; (b) the overlapping of sub-spectrum from two adjacent diffraction orders ($m = 53, 54$); (c) the overlapping of sub-spectrum from adjacent diffraction orders of 44 and 45; (d) the transmission of a single diffraction order of 44, which showed the minimized insert loss was 1.29 dB, and the adjacent crosstalk and noisy background were about 10 dB and 50 dB, respectively.

The designed AWG was simulated using a program based on beam propagation method (optiwaveBPM, Optiwave system Inc., Canada), and the result was shown in Fig. 4a. Here the spectrum was composed of eleven sub-spectra, and each one possessed the same diffraction order, which was from 44 to 54, respectively. The overlapping of spectrum between adjacent diffraction orders was unavoidable in order to form a continuous spectrum from 800–1000 nm. The maximum overlapping happened between the diffraction order of 53, 54, which was shown in Fig. 4b. The minimized overlapping occurs between the diffraction order of 44, 45 (Fig. 4c). This overlapping caused some pixels in the final 41 × 11 spots array had the same wavelength, which can be translated to a normal spectrum by a simple algorithm. The spectrum with diffraction order of 44 was shown in Fig. 4d. Here, the insert loss ranged from 1.29 dB in central output waveguide to 5.73 dB in the output waveguide in edge, and the adjacent crosstalk and noisy background were about 10 dB and 50 dB, respectively.

SIMULATION OF THE CROSS-DISPERSER

An optical design program (ZEMAX, Radiant Zemax, LLC, USA) was used to evaluate the image quality of the cross-disperser. A two dimensional model of this cross-disperser was shown in Fig. 5. It included three components: a parabolic-shape micro mirror, a prism and a reflective mirror in order to fold the optic path. Light from the output waveguide of AWG was collimated by the parabolic-shape micro mirror, dispersed by the prism, and finally imaged into a CCD.

The micro mirror array was prepared directly on the AWG wafer by micro-fabrication technology. Firstly, an aluminum 200 nm thick layer was deposited and patterned on top of the output waveguides of AWG as a hard mask in the following dry etching process. Next, a layer of SU-8 was spin-coated and patterned to leave a rounded hole. Following that, the unprotected silicon oxynitride as well as a layer of underneath silicon were removed by dry etching process (Fig. 6a). A photoresist (AZ 4620, Shipley, USA) was spin-coated on the wafer at a series of spinning speed and partly filled the round hole. Following hard bake, another layer of aluminum about 200 nm thick was evaporated on the wafer to realize a micro mirror (Fig. 6b). The profile of the micro mirror was mea-

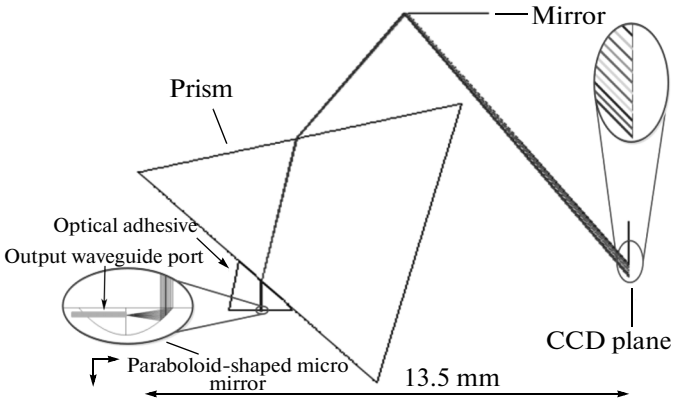

Fig. 5. The schematic diagram of the cross-disperser.

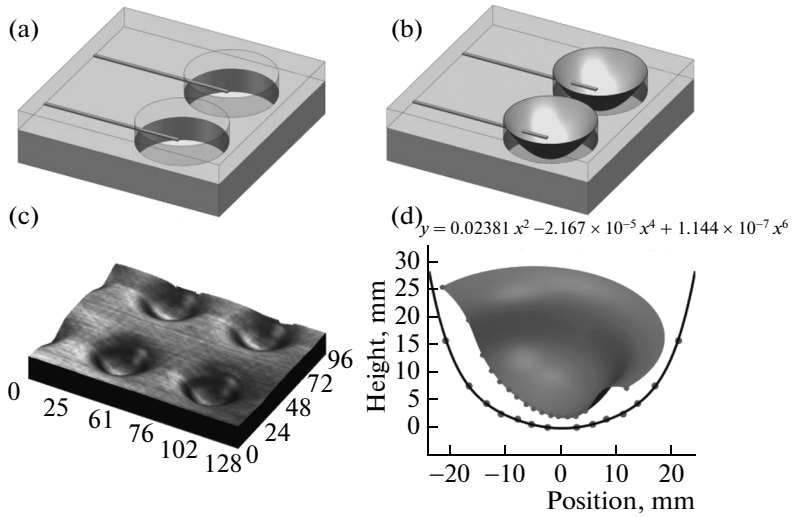

Fig. 6. The schematic diagram of the micro mirror: (a) a rounded hole was prepared around the end of the output waveguide; (b) after photoresist spin-coating and aluminum deposition, a micro mirror was formed at the front of the end of waveguide; (c) the profile of the micro mirror was measured by a laser conformal microscope; (d) the fitted equation revealed a parabolic-shape profile.

sured using a three dimensional laser conformal microscope (OLS1200–FAR2, Olympus) and was shown in Fig. 6c. A parabolic-shape profile was demonstrated at a spinning speed of 8000 rpm in the experiment and the measured profile as well as the fitted equation was shown in Fig. 6d. The thickness of the SU-8 layer and the depth of rounded hole were optimized to make the end of the output waveguide located exactly on the focal point of the paraboloid.

The profile of the micro mirror was input into ZEMAX program along with the parameters of the prism and the optical adhesive. Because each output waveguide has the similar feature, only the central output waveguide was simulated. As shown in Fig. 7, the image on the CCD receiving plane included eleven spots, and the size of these dispersed spots was about 10 μm, while the minimized gap between these spots was about 31 μm. These spots came from the eleven diffraction orders in the output waveguide, respectively, and their wavelength interval was in the range of 14.4 to 22.4 nm. Considering the interval space of the output waveguides was 50 μm, much larger than the spots size, the simulation result demonstrated the complete dispersion of input light.

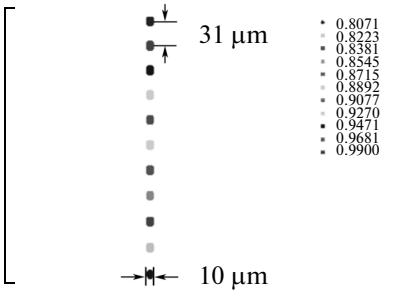

Fig. 7. The image quality after cross dispersion of the central output waveguide, which contains eleven different diffraction orders.

Theoretically, the insert loss of the micro mirror depends on the reflectivity and roughness of the aluminum surface. The loss of a 45° polymer micro mirror was reported to be 0.43 dB at 830 nm wavelength in a previous publication [25]. Considering additional high reflective aluminum film was coated on the parabolic-shape micro mirror, the loss should be less than this reported value. Since the transmission of the prism and the optical adhesive was more than 99% in 800–1000 nm range, the estimated loss of the cross-disperser is less than 0.5 dB. Taking account of this loss, the overall transmission of the combined dispersive device was shown in Fig. 8. Here, the insertion loss was about 1.79–8.34 dB at a spectral range of 800–1000 nm.

CONCLUSION

In this paper, a combined dispersive device including an AWG with multiple diffraction orders and a cross-disperser was proposed to realize a broadband, high spectral resolution Raman spectrometer. As a demonstration of this concept, a 41-channel AWG with eleven diffraction orders was designed and simulated, which showed a 0.55 nm spectral resolution in a spectral range of 800–1000 nm. The cross-disperser composed of a parabolic-shape micro mirror array and a prism was designed to further disperse the lights with multiple diffraction orders in each output waveguide. Using ZEMAX program, the simulation result demonstrated the complete dispersion of the light into a 41 × 11 pixels array on CCD. The volume of combined dispersive device was about 33 × 10 × 13 mm, and its overall insertion loss was about 1.79–8.34 dB. Accord-

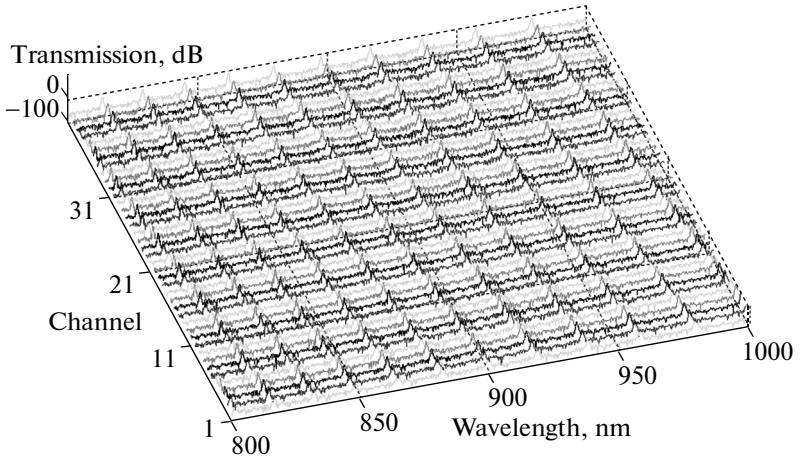

Fig. 8. The overall transmission of the combined dispersive device.

ingly, this dispersive device is believed to be promising for low cost handheld Raman spectrometer.

ACKNOWLEDGMENTS

This work was supported by NSFC under the project no. 21127001 and Ministry of Science and Technology of People's Republic of China under the project no. 2011YQ03012407.

REFERENCES

1. Y. Komai, H. Nagano, K. Okamoto, and K. Kodate, Jpn. J. Appl. Phys. **45** (8B), 6742 (2006).
2. K. Kodate and Y. Komai, J. Opt. A: Pure Appl. Opt. **10**, 044011 (2008).
3. P. Cheben, J. H. Schmid, A. Delage, et al., Opt. Express **15** (5), 2299 (2007).
4. N. Ismail, A. C. Baclig, P. J. Caspers, F. Sun, K. Wörhoff, R. M. de Ridder, M. Pollnau, and A. Driessen, in *Conference on Lasers and Electro-Optics (CLEO)* (San Jose, California, 2010), p. CFA7.
5. N. Cvetojevic, J. S. Lawrence, S. C. Ellis, J. Bland-Hawthorn, R. Haynes, and A. Horton, Opt. Express **17** (21), 18643 (2009).
6. V. D. Nguyen, B. I. Akca, K. Wörhoff, et al., Opt. Lett. **36** (7), 1293 (2010).
7. L. Chang, B. I. Akca, G. Sengo, K. Wörhoff, R. M. de Ridder, and M. Pollnau, in *Conference on Lasers and Electro-Optics (CLEO)* (San Jose, California, 2012), p. 34-JTh2A.
8. S. Murugkara, I. De Leon, Z. Shi, G. Lopez-Galmiche, J. Salvail, E. Ma, B. Gao, A. C. Liapis, J. E. Vornehm, and R. W. Boyd, in *Proceedings of SPIE* (San Francisco, California, 2012), p. 82640T-1.
9. N. A. Yebo, W. Bogaerts, Z. Hens, and R. Baets, in *Proceedings of SPIE* (San Francisco, California, 2012), Vol. 8264, p. 82640P-1.
10. N. A. Yebo, W. Bogaerts, Z. Hens, and R. Baets, IEEE Photonic Tech. L **23** (20), 1505 (2011).
11. N. Ismail, F. Sun, G. Sengo, K. Wörhoff, A. Driessen, R. M. de Ridder, and M. Pollnau, in *Conference on Lasers and Electro-Optics (CLEO)* (Baltimore, Maryland, 2011), p. CFN4.
12. B. I. Akca, N. Ismail, F. Sun, A. Driessen, K. Wörhoff, M. Pollnau, and R. M. de Ridder, in *Conference on Lasers and Electro-Optics (CLEO)* (Baltimore, Maryland, 2011), p. JWA65.
13. N. Ismail, F. Sun, G. Sengo, K. Wörhoff, A. Driessen, R. M. de Ridder, and M. Pollnau, Opt. Express **19** (9), 8781 (2011).
14. N. Ismail, B. I. Akca, F. Sun, K. Wörhoff, R.M. de Ridder, M. Pollnau, and A. Driessen, Opt. Lett. **35** (16), 2741 (2010).
15. K. Takada et al., IEEE Photonic Tech. L **13** (6), 577 (2001).
16. B. Momeni, E. S. Hosseini, and A. Adibi, in *OSA/IPNRA/NLO/SL* (Honolulu, Hawaii, 2009), p. IMD2.
17. B. Momeni, A. A. Eftekhar, M. Badieirostami, J. Huang, M. Askari, S. Mohammadi, E. S. Hosseini, M. Soltani, and A. Adibi, in *OSA/FiO/LS/OPE* (Rochester, New York, 2006), p. FThL4.
18. B. Momeni, E. S. Hosseini, M. Askari, M. Soltani, and A. Adibi, Opt. Commun. **282** (15), 3168 (2009).
19. B. Momeni, E. S. Hosseini, and A. Adibi, Opt. Express **17** (19), 17060 (2009).
20. B. Momeni, E. S. Hosseini, and A. Adibi, in *Proceedings of SPIE* (San Francisco, California, 2010), Vol. 7609, p. 76090L-1.
21. B. I. Akca, C. R. Doerr, G. Sengo, K. Wörhoff, M. Pollnau, and R. M. de Ridder, Opt. Express **20** (16), 18313 (2012).
22. N. Ismail, L.-P. Choo-Smith, K. Wörhoff, A. Driessen, A. C. Baclig, P. J. Caspers, G. J. Puppels, R. M. de Ridder, and M. Pollnau, Opt. Lett. **36** (23), 4629 (2011).
23. J. Bland-Hawthorn, J. Lawrence, G. Robertson, et al., in *Proceedings of SPIE* (San Diego, California, 2010), Vol. 7735, p. 7735-23.
24. N. Cvetojevic, N. Jovanovic, J. Lawrence, M. Withford, and J. Bland-Hawthorn, Opt. Express **20** (3), 2062 (2012).
25. J-S. Kim and J.-J. Kim, IEEE Photonics Tech. Lett. **16** (3), 798 (2004).